PT19c, Another Nonhypercalcemic Vitamin D_2 Derivative, Demonstrates Antitumor Efficacy in Epithelial Ovarian and Endometrial Cancer Models

Nada Kawar, Shannon Maclaughlan, Timothy C. Horan, Alper Uzun, Thilo S. Lange, Kyu K. Kim, Russell Hopson, Ajay P. Singh, Preetpal S. Sidhu, Kyle A. Glass, Sunil Shaw, James F. Padbury, Nicholi Vorsa, Leggy A. Arnold, Richard G. Moore, Laurent Brard and Rakesh K. Singh

Genes & Cancer published online 30 October 2013
DOI: 10.1177/1947601913507575

Original Article

Genes & Cancer
XX(X) 1–11

DOI: 10.1177/1947601913507575
ganc.sagepub.com
SAGE

PT19c, Another Nonhypercalcemic Vitamin D_2 Derivative, Demonstrates Antitumor Efficacy in Epithelial Ovarian and Endometrial Cancer Models

Nada Kawar[1], Shannon Maclaughlan[2], Timothy C. Horan[1], Alper Uzun[3], Thilo S. Lange[1], Kyu K. Kim[1], Russell Hopson[4], Ajay P. Singh[5], Preetpal S. Sidhu[6], Kyle A. Glass[3], Sunil Shaw[3], James F. Padbury[3], Nicholi Vorsa[5], Leggy A. Arnold[6], Richard G. Moore[1], Laurent Brard[7], and Rakesh K. Singh[1]

Submitted 11-Mar-2013; accepted 12-Sep-2013

Abstract

Hypercalcemia remains a major impediment to the clinical use of vitamin D in cancer treatment. Approaches to remove hypercalcemia and development of nonhypercalcemic agents can lead to the development of vitamin D–based therapies for treatment of various cancers. In this report, *in vitro* and *in vivo* anticancer efficacy, safety, and details of vitamin D receptor (VDR) interactions of PT19c, a novel nonhypercalcemic vitamin D derived anticancer agent, are described. PT19c was synthesized by bromoacetylation of PTAD-ergocalciferol adduct. Broader growth inhibitory potential of PT19c was evaluated in a panel of chemoresistant breast, renal, ovarian, lung, colon, leukemia, prostate, melanoma, and central nervous system cancers cell line types of NCI60 cell line panel. Interactions of PT19c with VDR were determined by a VDR transactivation assay in a VDR overexpressing VDR-UAS-bla-HEK293 cells, *in vitro* VDR-coregulator binding, and molecular docking with VDR-ligand binding domain (VDR-LBD) in comparison with calcitriol. Acute toxicity of PT19c was determined in nontumored mice. *In vivo* antitumor efficacy of PT19c was determined via ovarian and endometrial cancer xenograft experiments. Effect of PT19c on actin filament organization and focal adhesion formation was examined by microscopy. PT19c treatment inhibited growth of chemoresistant NCI60 cell lines ($\log_{10}$GI50 ~ −4.05 to −6.73). PT19c (10 mg/kg, 35 days) reduced growth of ovarian and endometrial xenograft tumor without hypercalcemia. PT19c exerted no acute toxicity up to 400 mg/kg (QDx1) in animals. PT19c showed weak VDR antagonism, lack of VDR binding, and inverted spatial accommodation in VDR-LBD. PT19c caused actin filament dysfunction and inhibited focal adhesion in SKOV-3 cells. PT19c is a VDR independent nonhypercalcemic vitamin D–derived agent that showed noteworthy safety and efficacy in ovarian and endometrial cancer animal models and inhibited actin organization and focal adhesion in ovarian cancer cells.

Keywords

vitamin D, hypercalcemia, antitumor efficacy, ovarian cancer, endometrial cancer

Introduction

Calcitriol (1α,25(OH)$_2$D$_3$), the biologically active form of vitamin D$_3$, and its structural analogs have shown antiproliferative, apoptotic, pro-differentiation, and anti-angiogenic effects in many types of cancers.[1-3] Various clinical phase I/II trials have shown that hypercalcemia and other toxicities are the major impediment to the clinical use of vitamin D despite clinical responses.[3,4] Newer synthetic analogs such as EB1089[5] and Maxacalcitol[6] have demonstrated inhibitory effects in various solid tumors with reduced calcemic effects. Vitamin D–dependent hypercalcemia remains a major impediment for its development and a clinical tool for cancer treatment. The development of nonhypercalcemic vitamin D analogs is urgently needed.

Recently, we described the development of a new class of antitumor molecules via the modification of Vitamin D$_2$.[7-10] The heterocyclization of the A-ring diene structure of Vitamin D$_2$ via a known Diels-Alder reaction provided

Supplementary material for this article is available on the *Genes & Cancer* website at http://ganc.sagepub.com/supplemental.

[1]Molecular Therapeutics Laboratory, Program in Women's Oncology, Department of Obstetrics and Gynecology, Women and Infants' Hospital, Brown University, Providence, RI, USA
[2]Stanford Women's Cancer Center, Stanford University, Stanford, CA, USA
[3]Department of Pediatrics, Women and Infants' Hospital, Brown University, Providence, RI, USA
[4]Department of Chemistry, Brown University, Providence, RI, USA
[5]Department of Plant Biology and Pathology, Rutgers University, New Brunswick, NJ, USA
[6]Department of Chemistry and Biochemistry, University of Wisconsin, Milwaukee, WI, USA
[7]Department of Obstetrics and Gynecology, School of Medicine, Southern Illinois University, Springfield, IL, USA

Corresponding Author:
Rakesh K. Singh, Molecular Therapeutics Laboratory, Program in Women's Oncology, Department of Obstetrics and Gynecology, Kilguss Research Institute, Women and Infants' Hospital, Brown University, Providence, RI 02903, USA (Email: rsingh@wihri.org).

an intermediate tricyclic heteroatoms rich adduct scaffold that carried drug-like features. A limited library of α-haloalkyl acetates of adduct was synthesized and screened for anticancer activity in cultured ovarian, endometrial, prostate, and neuroblastoma cancer cell lines. Two lead molecules, MT19c[7-10] and PT19c, with potential anticancer activity were identified during screening. In this report, the design, synthesis (for chemical name, synthesis protocol, and characterization see Suppl. Section S1), cytotoxic functions, interaction with vitamin D receptor (VDR), safety, and *in vitro* and *in vivo* efficacy of PT19c in 2 independent xenograft animal models of platinum resistant ovarian cancer and hormone responsive endometrial cancer are described. Mechanistically, PT19c treatment causes catastrophic changes in actin filament organization in ovarian cancer (SKOV-3) and endometrial cancer (ECC-1) cells.

PT19c demonstrated growth inhibition of the NCI60 cell lines ($\log_{10}GI_{50}$ ~ −4.05 to −6.73) derived from melanoma, breast, ovarian, central nervous system (CNS), renal, leukemia, non–small cell lung, and prostate cancer. PT19c showed biologically very weak VDR antagonism in a cell-based reporter assay and showed no binding to VDR in a VDR-coactivator binding assay. A molecular docking simulation of PT19c with VDR-ligand binding domain (VDR-LBD) showed that PT19c acquires an inverted spatial accommodation in VDR-LBD contrary to calcitriol and, therefore, does not exert the classical calcitriol-VDR-LBD interactions. PT19c (10 mg/kg/35 days) reduced the growth of ovarian (SKOV-3) and endometrial (ECC-1) xenograft tumor models without hypercalcemia and showed no acute toxicity with doses up to 400 mg/bwt in animals. Mechanistically, PT19c caused actin rearrangement or condensation in SKOV-3 and ECC-1 cells, followed by apoptosis.

In summary, we describe a novel approach to design nonhypercalcemic vitamin D–derived antitumor agents (PT19c and MT19c) that exerted no interaction with VDR and did not cause hypercalcemia in animals. PT19c, the agent described in this article, showed excellent safety in animals and displayed noteworthy anticancer effects in platinum refractory ovarian cancer and hormone sensitive endometrial cancer xenograft animal models. PT19c treatment also revealed promising therapeutic potential in the treatment of breast, lung, CNS, melanoma, ovarian, and renal cancers in NCI-conducted hollow fiber assay.

Results

Synthesis and structural characterization of PT19c. The chemical modification of ergocalciferol via our short pathway process yielded 2 promising anticancer lead molecules (MT19c and PT19c). The core structure of this class of compounds was confirmed by single-crystal X-ray crystallography using MT19c. PT19c is the *N*-phenyl analog of MT19c and therefore possesses the same core structure. To further evaluate the chemical structure of PT19c, we conducted COESY and HETCOESY NMR experiments and other structural correlative studies described in Figure 1B or in the Supplementary Supporting Information section.

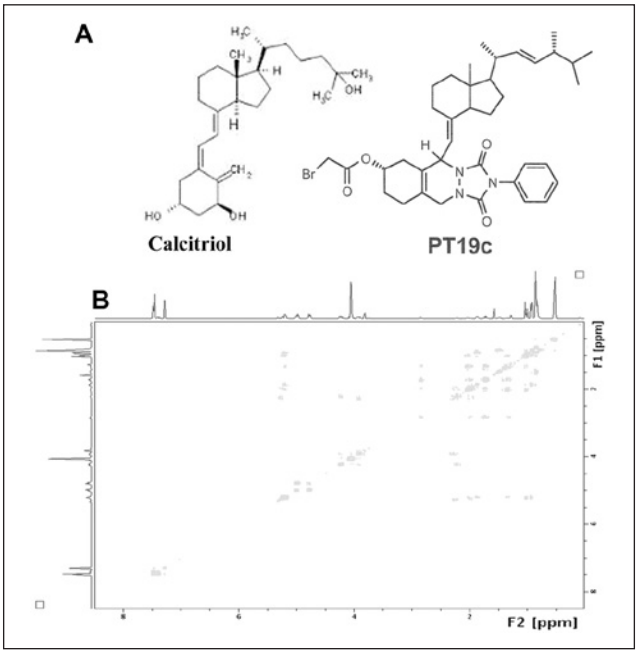

Figure 1. (**A**) Chemical structures of calcitriol and PT19c. For the synthesis and characterization data, refer the Supplementary Supporting Information. (**B**). The HETCOSY NMR profile depicts the key interactions of protons in PT19c with heteroatoms.

PT19c does not affect VDR transcription in cells and is a very weak VDR antagonist. To evaluate transcriptional regulation of VDR in cells on PT19c treatment, we employed a cell-based functional-VDR-reporter assay (GeneBLAzer Technology, Invitrogen, Carlsbad, CA), using transformed HEK293 cells that express a fusion protein of VDR-LBD-GAL4 DNA-binding domain, which is activated by calcitriol and induces transcription of a β-lactamase reporter gene. The transcriptional activation of VDR in the presence of PT19c was determined after 5-hour treatment with the control calcitriol (0.1 pM to 1 nM) (Fig. 2A; upper panel) or PT19c (1 nM to 1,000 μM) (Fig. 2A; middle panel). Calcitriol caused VDR activation at 10 pM (IC_{50} ~30 pM). PT19c showed no agonistic activity at the concentrations tested. To analyze antagonistic effects, cells stimulated by calcitriol (120 pM) were treated with PT19c (1 nM to 50 μM) (Fig. 2A; lower panel) for 5 hours. PT19c inhibited calcitriol-induced VDR activation only at relatively high concentrations (IC_{50} ~100 μM). Thus, PT19c showed an extremely weak VDR antagonistic effect unlikely to have biological consequence. PT19c is an approximately 1,000

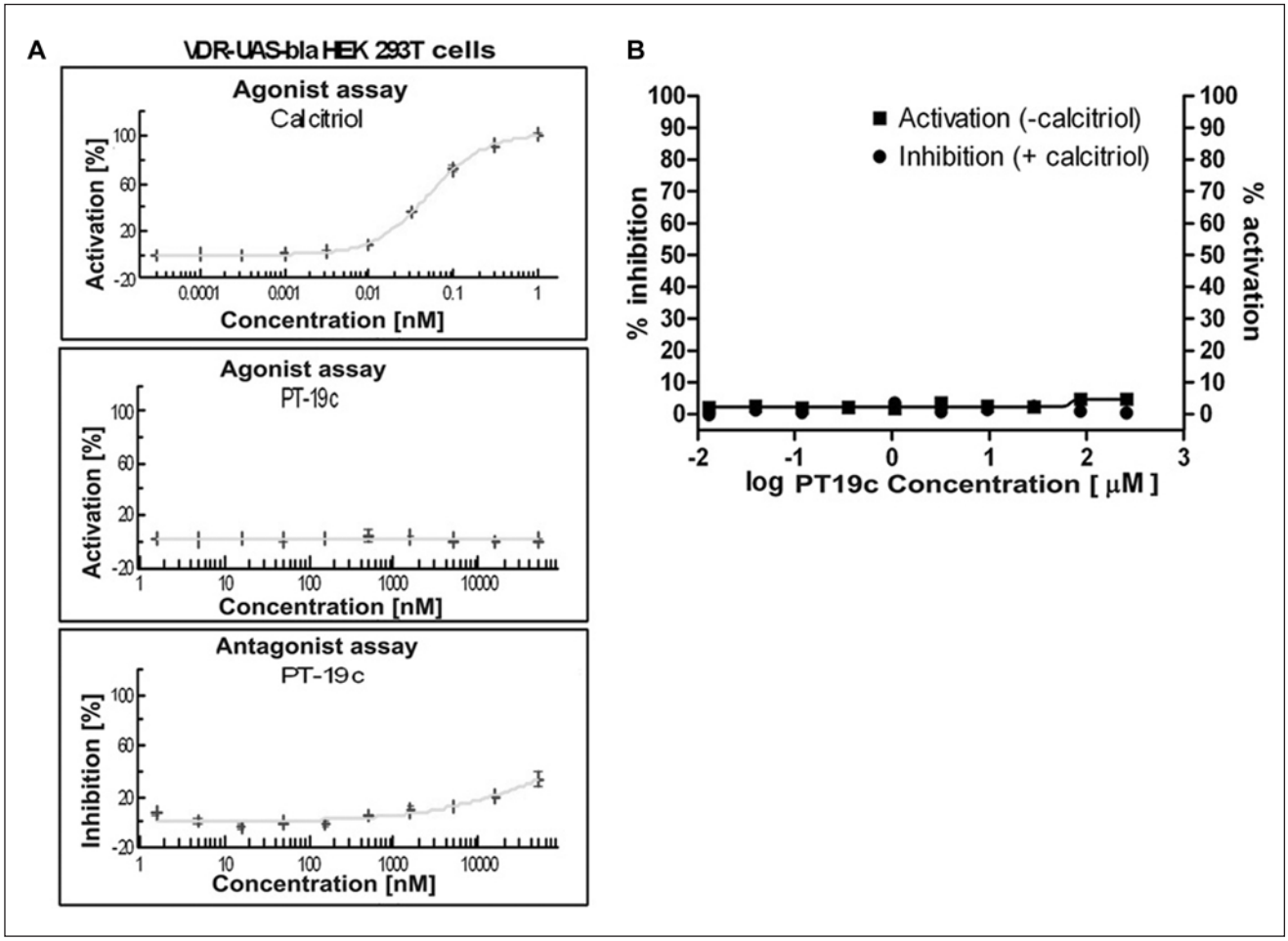

Figure 2. (**A**) VDR agonist or antagonist screening of PT19c. VDR overexpressing VDR-UAS-bla HEK 293T cells were treated for 5 hours with calcitriol/vitamin D_3 (0.1 pM to 1 nM; **left panel**) or PT19c (1 nM to 1 mM; **middle panel**) and VDR activation was analyzed. To analyze antagonistic effects the assay was carried out (SelectScreen Cell-based Nuclear Receptor Profiling Services, Invitrogen) after cell stimulation with calcitriol/vitamin D_3 (120 pM) and treatment with MT19c (1 nM to 1 mM; **right panel**) for 5 hours. (**B**) VDR-coactivator binding assay. VDR-LBD and fluorescently labeled coactivator peptide SRC2-3 was treated with different concentrations of PT19c in the presence ● (% inhibition) and absence ■ (% activation) of calcitriol (100 nM). Data were determined using fluorescence polarization and normalized to calcitriol (100% activation), (100% inhibition), and vehicle DMSO.

times less potent VDR antagonist than TEI-9647 or ZK159222.[11]

The biochemical interactions between PT19c and VDR were investigated using a fluorescence polarization assay.[9] PT19c was incubated with VDR-LBD and a fluorescent labeled coactivator peptide (SRC2-3) in the presence and absence of calcitriol. In the presence of agonist calcitriol, VDR is able to interact with the coactivator peptide SRC2-3; on the other hand, VDR antagonists disrupt this interaction by a direct or allosteric mode of inhibition. PT19c showed a very weak antagonistic effect at a concentration of >50 μM (Fig. 2B) and full inhibition did not occur at a concentration of 1 mM. Similarly, the ability of PT19c to bind to VDR and initiate the conformational change of VDR to allow coactivator recruitment was determined in the absence of calcitriol. Our results clearly show that PT19c is not a VDR agonist (Fig. 2B).

Effects of PT19c on serum calcium levels in animals and acute toxicity determination of PT19c. Calcitriol and other vitamin D analogs cause hypercalcemia in animals and humans at therapeutic concentrations. We investigated if PT19c treatment induced hypercalcemia in mice despite its structural alteration of the A-ring and conjugated diene in ergocalciferol. Nude mice were randomly assigned to control, PT19C, and calcitriol treatment groups as described in the Materials and Methods section. In the control group, the mean serum calcium level after 35 days of treatment was ~10.0 mEq/dL (Fig. 3A). Calcitriol treatment at 10 μg/kg dose resulted in hypercalcemia, with serum calcium levels

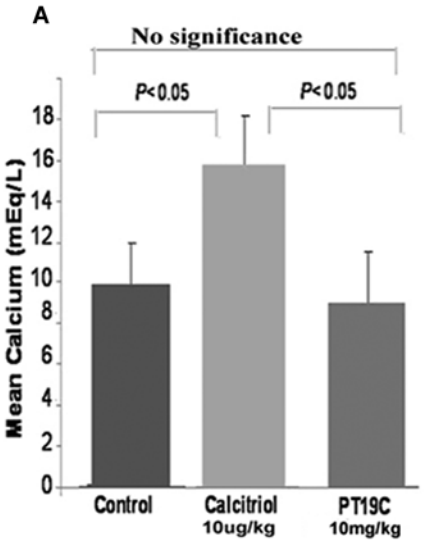

B

Nontumored Animal Toxicity assay for PT19c

Host: Nude mice, Sex: F

Treatment Drug	Dose	Route	Schedule	Death day	Survival	day
PT19c	400mg/kg	IP	QDx1, Day-0	none	1/1	13
PT19c	200mg/kg	IP	QDx1, Day-0	none	1/1	13
PT19c	100mg/kg	IP	QDx1, Day-0	none	1/1	13

Vehicle: in 10% DMSO in saline/Tween 80, Inj. Vol: 0.05ml/10gm bwt

Figure 3. Serum calcium levels in mice after PT19c treatment. (**A**) 8 mice each were treated with PT19c and 8 were treated with vehicle for 35 days, blood collected, and serum calcium analyzed. Change in mean serum calcium was compared between groups by Student's *t* test with unequal variances (**B**) Nontumoral toxicity in animals. Mice were treated with 400, 200, and 100 mg per the schedule and route shown. The animals were observed for death till the 13th day. For details of this acute toxicity assay, see http://dtp.nci.nih.gov.

reaching ~16 mEq/L. In the PT19c treatment group at doses of 10 mg/kg bwt, serum calcium levels was normal (~9 mEq/dL) and did not significantly differ from the control group (Fig. 3A). The serum calcium levels between control and calcitriol or PT19c and calcitriol differed significantly ($P < 0.05$). Calcitriol treated mice demonstrated weight loss, skin changes, decreased appetite, and lethargy.

In addition to being nonhypercalcemic, PT19c treatment did not exert acute toxicity in animals during the 13 days of observation in a nontumored nude mice model based acute toxicity assay conducted by the National Cancer Institute. Test animal did not die even at a high dose of 400 mg/kg. At the present tested dose PT19c is one of the safest anticancer agents described in the literature.

Molecular docking simulation (MDS) of VDR and PT19c interaction. As shown earlier, PT19c did not affect VDR transcription in cells and showed biologically inconsequential VDR antagonism. To investigate the molecular causes for the lack of interaction with VDR, we conducted a MDS of VDR with PT19c. The molecular docking of PT19c with VDR was compared with VDR liganded to calcitriol (PDB ID: 1DB1) utilizing the AutoDock 4.0 program.[12] A series of possible protein-ligand complexes were chosen based on their binding free-energy. The lowest docked energy conformation was chosen as the model candidate for studying the docking of PT19c with VDR. The amino acids interacting with calcitriol in VDR-ligand binding domain (VDR-LBD) were used as a reference for determination of PT19c interactions. Figure 4 depicts the MDS for VDR and calcitriol (Fig. 4A and C, left panels) or PT19c docked with VDR (Fig. 4B and D, right panels). We observed that PT19c acquired an inverted accommodation in VDR-LBD compared to calcitriol. Molecular docking shows that inverted entry of PT19c in the narrow binding domain of VDR-LBD distorts the ligand-binding domain and key biological amino acid interactions (e.g., His397) required for VDR-regulator signaling.

PT19c treatment inhibits the proliferation of chemoresistant NCI60 cancer cell lines. Based on encouraging in-house *in vitro* cytotoxicity data of PT19c against a panel of ovarian (SKOV-3, OVCAR-8, IGROV-1, and CaOV-3) and endometrial (ECC-1 and KLE) cancer cell lines (data not shown), PT19c was submitted to the Developmental Therapeutic Program for broader screening against 60 cell lines of the National Cancer Institute. The NCI60 cell lines are derived from leukemia, non–small cell lung cancer, renal, breast, prostate, melanoma, ovarian, CNS, and colon cancers in humans.

PT19c showed broad cytotoxic effects, and comparison of growth inhibition GI_{50}, TGI, and LC_{50} revealed cell-type and tumor-type specificity in the effectiveness of PT19c against chemoresistant cancer cell lines derived from 9 different tissue types in a NCI60 cell line screen (Fig. 5) (for details refer http://dtp.nci.nih.gov). The melanoma, small

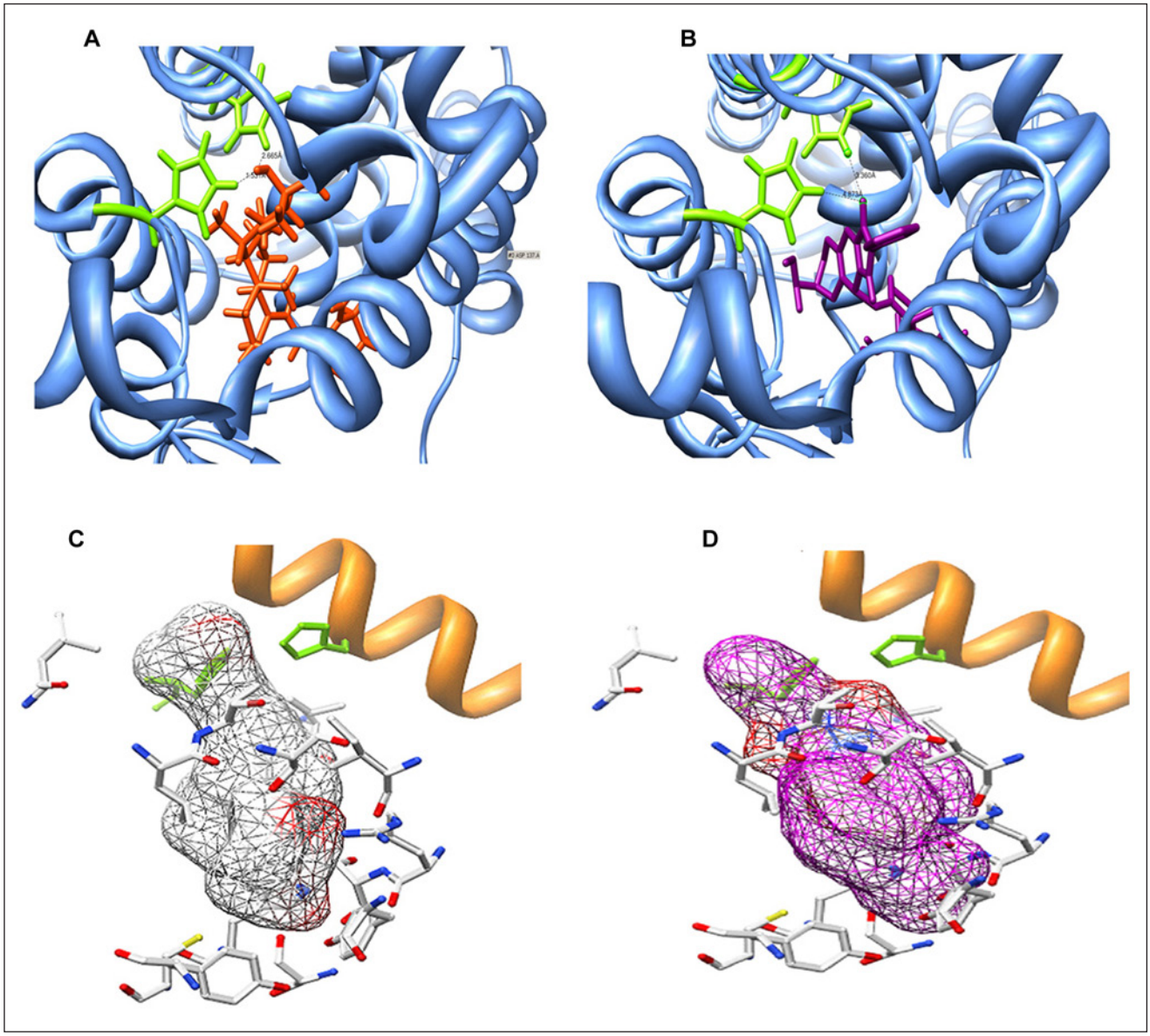

Figure 4. Molecular docking simulation of VDR and PT19c. (**A**) 3D structures of VDR/calcitriol and VDR/PT19c complexes. **Left panel:** VDR/calcitriol complex (calcitriol in center, helix 11 = white color). **Right panel:** VDR/PT19c complex (PT19c in center, 11 = light green). MDS was carried out using the AutoDock 4.0 program with the structure of PT19c and calcitriol-liganded VDR provided by the Protein Data Bank. Images of structures were generated using UCSF Chimera. (**B**) Sequence of VDR ligand binding site. Blue color code represents helices in the structure. Green color code represents amino acids with direct interaction to the ligand (calcitriol). (**C**) Interaction comparison. **Left panel:** Interaction between Leu227 and calcitriol. (**D**) **Right panel:** Interaction between Leu227 and PT19c.

cell lung cancer, and renal and breast cancer cells were highly sensitive to PT19c treatment. Cell lines of leukemia, CNS, ovarian, colon, and prostate were up to 1 to 2 log fold resistant to PT19c treatment. Though relatively resistant, these cancer cell lines still showed response to PT19c treatment at or below ~10 μM concentration.

PT19c treatment suppressed the growth of ovarian and endometrial cancer xenografts in nude mice. The antitumor efficacy of PT19c (10 mg/kg bwt) was evaluated using human EOC SKOV-3 cell and hormone refractory endometrial cancer (ECC-1) cell line derived xenografts in nude (NU/NU) mice over a period of 35 days (Fig. 6 and Fig. 7). To evaluate the therapeutic efficacy of PT19c against platinum resistant ovarian cancer, nude mice were xenografted with SKOV-3 cells as described in the Materials and Methods section. SKOV-3 cells are characterized platinum resistant phenotype of serous ovarian cancer (Manassas, VA).

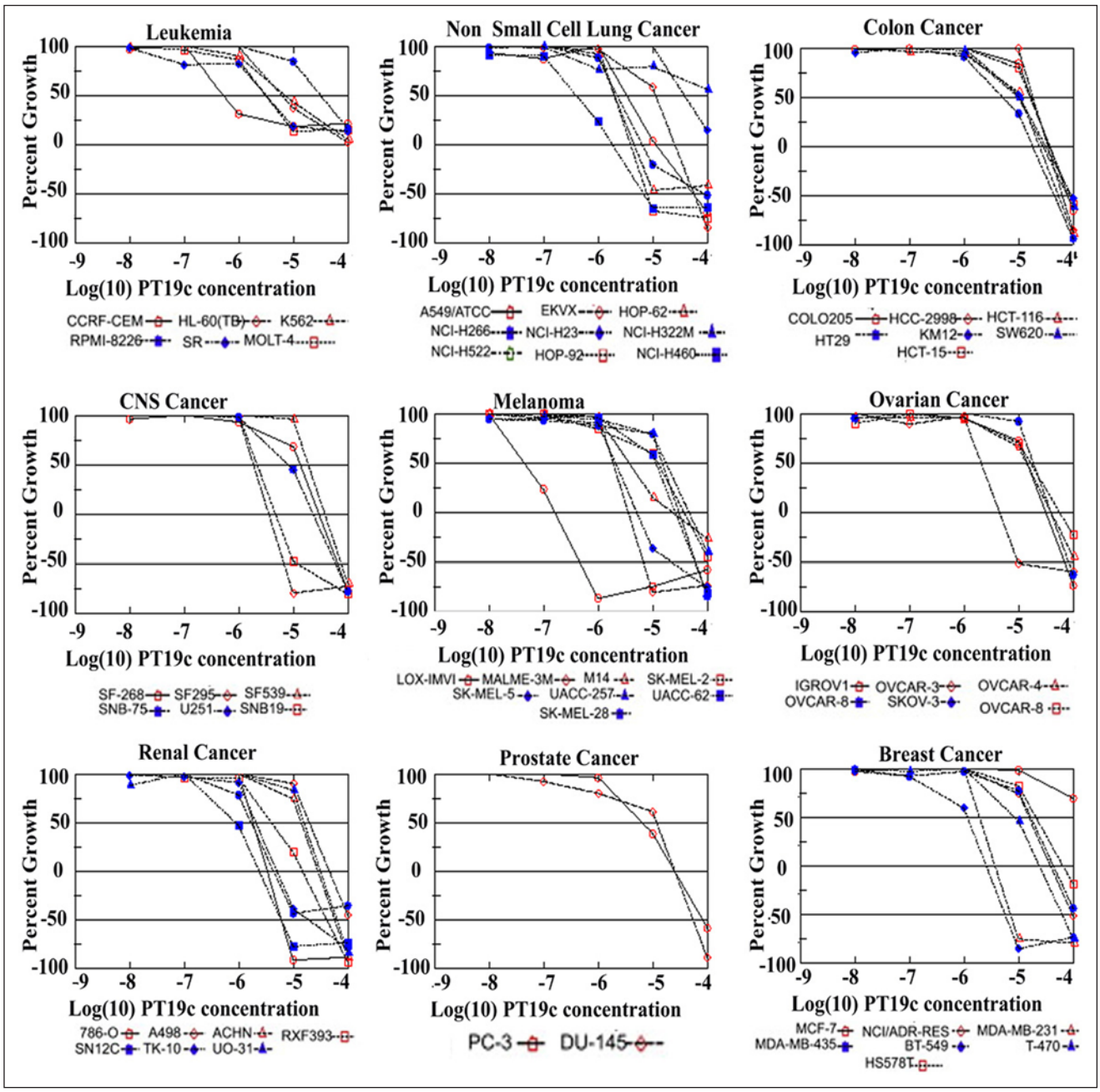

Figure 5. *In vitro* growth inhibition of NCI60 cell lines. Cell lines were treated with PT19c (log −9 to −4 molar concentration) or vehicle. Percent growth inhibition (GI) values are shown.

PT19c treatment significantly reduced the progression of established xenograft tumors in nude mice during the trial ($P = 0.04$) (Fig. 6A) while the vehicle treated animals showed regular increase in tumor size. We also observed that PT19c treated animal showed relatively slower gain in weight compared to vehicle treated ovarian tumor animals ($P < 0.0001$) (Fig. 6B).

The efficacy of PT19c was also evaluated in a hormone responsive endometrial ovarian cancer xenograft model. In this assay, we also employed calcitriol as positive control and compared the efficacy of PT19c with calcitriol. As the trial progressed, the xenograft tumor size in the animals treated with vehicle continued to increase. In the PT19c treatment group, tumor size decreased considerably during

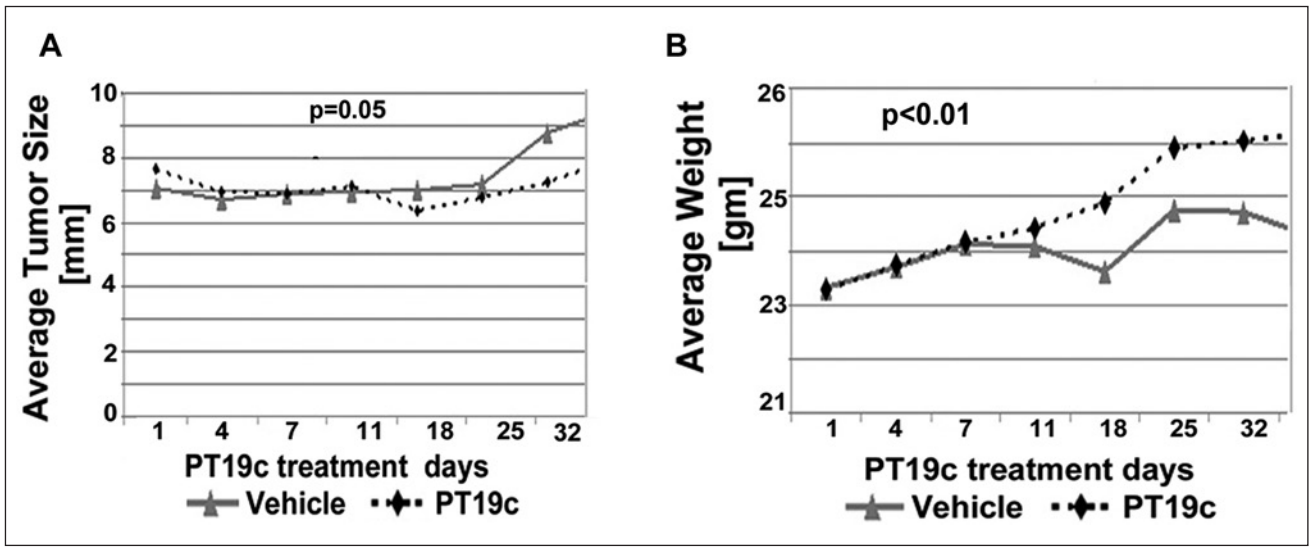

Figure 6. (**A**, **B**) Efficacy of PT19c in epithelial ovarian cancer model. Nude mice bearing SKOV-3 derived tumor xenografts were dosed (IP) with either overall time difference via Linear Mixed Effects Regression (LMER) analysis vehicle control (n = 8) or PT19c (10 mg/kg) (n = 8) on alternate days for 35 days. Tumor size and weight were recorded using a caliper every 5 days.

the last 15 days of treatment ($P < 0.001$) (Fig. 7A). Two of 8 animals exhibited nearly complete response and the remaining 6 animals experienced a partial response to PT19c treatment. On the other hand, calcitriol treatment definitely slowed the endometrial tumor growth significantly ($P < 0.0001$) but tumor size increased continuously in animals carrying endometrial ECC-1 cell xenografts (Fig. 7C). None of the animals treated with calcitriol showed either a partial or complete response. Calcitriol treated animals showed excessive hypercalcemia in serum and were found to be highly morbid and lost weight considerably during the trial (Fig. 7D) ($P < 0.0001$), whereas the PT19c treated animals showed minor weight gain as the treatment progressed ($P < 0.0001$) (Fig. 7B).

PT19c treatment caused actin filament dysfunction in SKOV-3 cells. PT19c treatment of SKOV-3 ovarian cancer cells caused profound changes in the focal adhesion formation and actin filament organization in SKOV-3 cells and ECC-1 cells within 24 hours (Fig. 8). While control cells showed characteristic focal adhesion formation and actin arrangement (arrows) in the cells, PT19c (5 μM) treatment caused strong actin remodeling such as actin retraction, tear, and condensation followed by cellular disintegration and death.

Discussion

Calcitriol and other vitamin D analogs have long been investigated in many human clinical trials to treat a variety of human cancers.[1] Many clinical trials evaluating the use of calcitriol in combinational therapy are still ongoing. However, hypercalcemia, hypercalciuria, and hyperphosphatemia have consistently been identified as the major impediments to their clinical use. Classical vitamin D biological functions mediated by carbon-1 and carbon-25 of calcitriol have been linked to hypercalcemia seen with these agents.[2]

To elaborate further on the role of the A-ring in hypercalcemia in animals, we modified the A-ring of vitamin D_2 to disable 1α-hydroxylase interactions elicited by the A-ring. On construction of a bulkier tricyclic heterocyclic ring, and further bromoacetylation to generate PT19c and MT19c,[7-10] we found that hypercalcemia was no longer associated with these compounds in animals. This chemical structure–based elucidation confirmed that the A-ring of the vitamin D and related analogs indeed plays a central role in hypercalcemia since PT19c treatment devoid of the natural A-ring structure did not cause hypercalcemia in animals during 35 days of animal trial. On the contrary, treatment with calcitriol (10 μg/kg) elevated serum calcium levels in animals to the levels of ~16 mEq/L by the 35th day of treatment and caused serious debilitations and morbidities among the animal subjects.

Further elaboration of the interaction of PT19c with VDR was conducted to secure the possible explanation for nonhypercalcemia in animals despite up to 1,000-fold higher drug treatment compared to calcitriol. PT19c did not show any biologically relevant binding, agonist or antagonist, of VDR protein in fluorescence VDR SRC-3 coactivator assay. Similarly, PT19c did not activate or antagonize VDR in a cell-based VDR transactivation reporter assay in

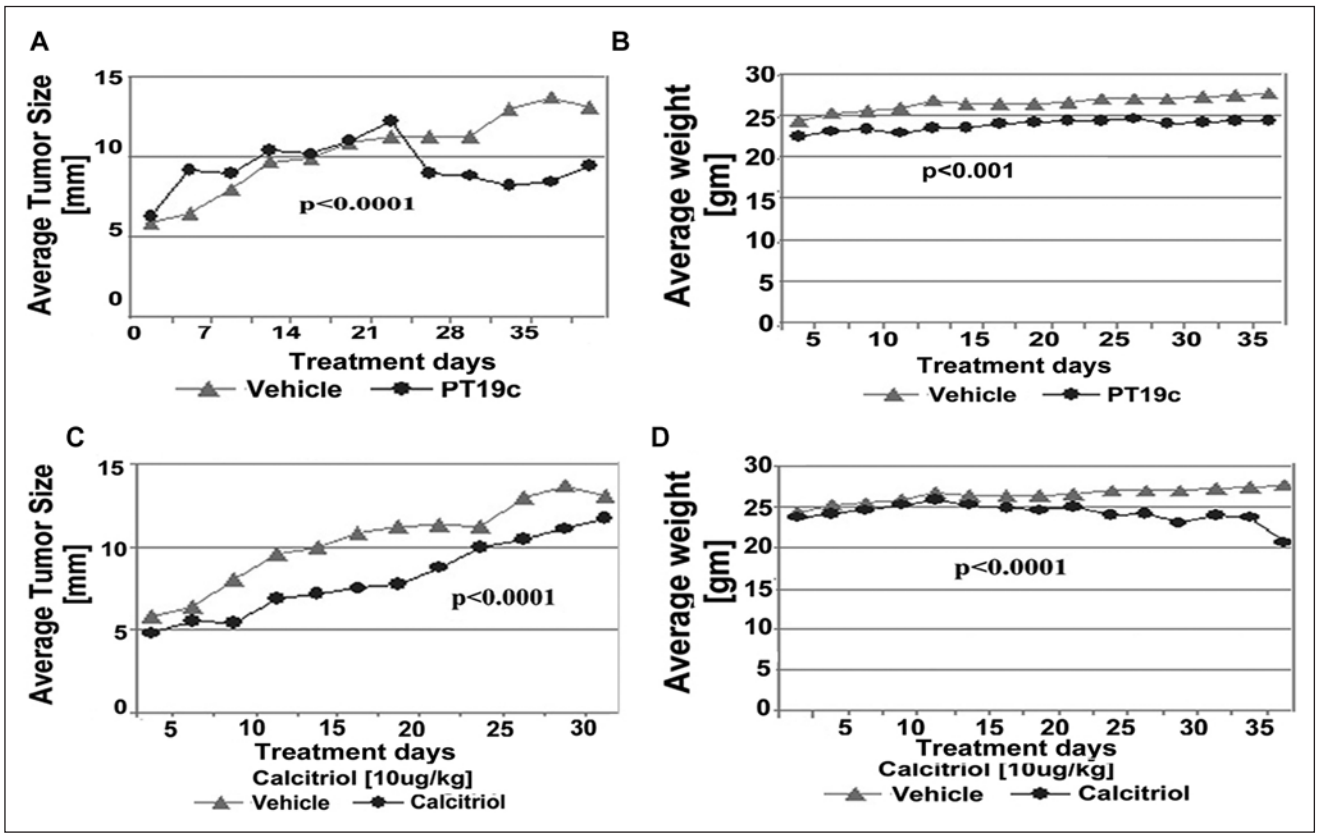

Figure 7. (**A**-**D**) Anticancer activity of PT19c in an endometrial cancer model in mice. Nude mice (16 treated and 8 controls) bearing ECC-1 derived tumor xenografts were treated IP with either vehicle control or PT19c (10 mg/kg bwt) (n = 8) or calcitriol (10 μg/kg bwt) (n = 8) on alternate days for 35 days. Tumor size and weight were recorded using a caliper every 5 days. The statistical significance was determined by ANOVA. Linear mixed effect regression (LMER) indicating overall time differences. Note: A recent article by Korch *et al.*[13] suggests that ECC-1 cells are Ishikawa cells that are contaminated with MCF-7 cells.

VDR overexpressing HEK293 cells. The reason for such a passivity of PT19c with VDR was identified via a MDS conducted with VDR-ligand binding domain *in silico*. PT19c entered VDR-LBD in an opposite manner to calcitriol. This reverse accommodation of PT19c in VDR-LBD disabled the typical calcitriol-VDR interactions. The inverse accommodation of PT19c in VDR-ligand binding domain had the following consequences: (a) in place of calcitriol C-25 (Fig. 4A), the tricyclic ring of PT19c situated itself between helices 11 and 12 in the VDR-LBD[11] (Fig. 4B); (b) carbonyl oxygen atom of PT19c displayed stronger hydrogen binding with VDR residue H397 (2.05 Å) (Fig. 4D) compared to the 25-hydroxy group of calcitriol (2.8 Å) (Fig. 4C); and (c) PT19c disrupted the natural orientation of helices 11, 12, and 13 on inverted entry in the VDR-LBD. PT19c therefore disabled VDR-coactivator interactions essential for VDR signaling. On the contrary, calcitriol as shown in Figure 4 stabilizes helix-11/13 interaction with VDR-coactivator SRC2-3 to enact the genomic functions of VDR. Taken together, our molecular design approach reveals that PT19c is neither a strong agonist nor an antagonist and therefore does not dock/interact with VDR, suggesting a possibility that other receptors might be involved in anticancer effects of PT19c.

PT19c demonstrated potent dose dependent and cell line selective growth inhibition of the chemoresistant cell lines enlisted in the NCI60 cell line panel in low micromolar ranges (GI_{50} ~1-10 μM).[13] Similarly, PT19c treatment for 35 days, treated alternate days intraperitoneally, resulted in the significant reduction of the progression and tumor burden compared to the vehicle group ($P < 0.05$) and majority of the animals showed partial to nearly complete response without any observable toxicity. Moreover, PT19c treatment showed growth inhibition of endometrial cancer xenograft derived from hormone responsive ECC-1 cells ($P < 0.0001$). The majority of the animals showed partial response, and 2 animals showed complete response to the therapy. PT19c treated animals showed good health and no observable toxicity was recorded. On the other hand, calcitriol treatment slowed the progression of the tumors initially, but the tumor continued to grow. Additionally, calcitriol treatment caused debilitative levels of serum

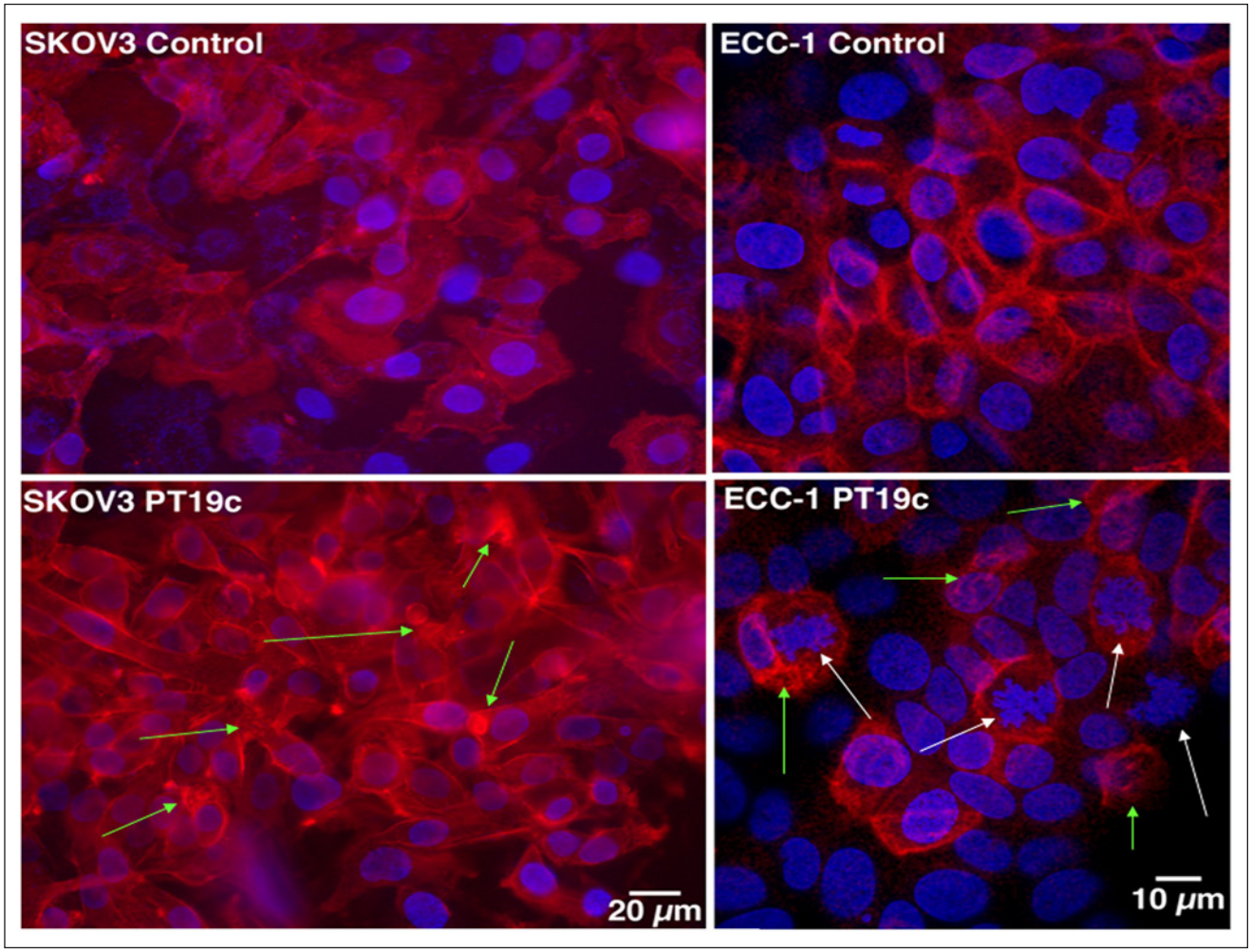

Figure 8. The effect of PT19c on the focal adhesion and actin assembly. SKOV-3 and ECC-1 (20,000) cells were seeded in glass chamber slides and treated with PT19c (5 μM) for 24 hours. The cells were fixed, washed, and stained with alexafluor-phalloidin. Green arrows indicate actin disruptions and white arrows indicate chromatin destruction. The images were recorded by an inverted precooled camera (40× magnification).

calcium elevation and animals presented with lethargy, skin changes and weight loss.

In addition to excellent efficacy, lack of hypercalcemia and other deleterious effect on the health of the animals during repeated animal trials, PT19c demonstrated noteworthy safety in an acute toxicity assay conducted by the Developmental Therapeutics Program of the National Cancer Institute (NCI). PT19c treatment did not cause death or any observable toxicity in mice till 13 days of trial even at a remarkably higher dose of 400 mg/kg (Fig. 3B).

The molecular targets and mechanism of action of PT19c are being elucidated in our laboratories. Our studies indicate that PT19c treatment can cause catastrophic changes in the focal adhesion formations and actin filament organization including actin condensation (Fig. 7). Actin undergoes rapid polymerization and depolymerization to maintain morphological plasticity of living cells including cancer cells.[14] It has been shown that apoptosis and cell death can result if actin polymerization was blocked and existing actin filaments assembly were disturbed, for example, due to treatment with cytochalasins.[15-17] Similarly, Suria *et al*. observed that cytoskeletal disruption by cytochalasin causes apoptosis mediated by ICE-like and caspase-3.[18] Further studies aimed at understanding the impact of PT19c on the actin disarrangement in the cancer cells are continuing in our laboratory to ascertain whether inhibition of focal adhesion formation and actin filament organization is the central mechanism of action of PT19c *in vitro* and *in vivo*, and whether inhibition of focal adhesion formation and causing actin catastrophe is a viable therapeutic approach to treat epithelial ovarian cancer or endometrial cancer.

Materials and Methods

Synthesis of PT19c, reagents, and cell culture. The details of the synthesis and structural characterization of PT19c are

described in the Supplementary Information section (S-1). Briefly, commercially available ergocalciferol underwent a Diels-Alder reaction with *N*-phenyl-1,2,4-triazolinedione to generate an adduct (Suppl. Fig. 1A; structure 2), which on reaction with bromoacetic acid in the presence of DCC (*N,N′*-dicyclohexylcarbodiimide) generated PT19c in good yield (Fig. 1A). The structure of PT19c was confirmed by COESY and NOESY NMR experiments, and the purity was assessed by high performance liquid chromatography. The PT19c product utilized in this study was 99% pure.

Human ovarian epithelial adenocarcinoma cell line SKOV-3 and endometrial cancer cells ECC-1 were obtained from American Type Culture Collection ATCC (Manassas, VA). All cells were seeded at 5×10^5/T75 flask (Corning, Inc, Corning, NY) and cultured to ~80% confluence according to the supplier's recommendations. For all assays, cells were seeded in complete DMEM media and allowed to attach overnight. Calcitriol was purchased from Alexis Corporation, (Farmingdale, NY) and dissolved in EtOH for experimental uses. Note: a recent article by Korch *et al*.[13] suggests that ECC-1 cells are Ishikawa endometrial cancer cells and/or contaminated with MCF-7 cells

NCI 60 cancer cell line assay and acute toxicity studies in animals. PT19c was screened through the National Cancer Institute (NCI60 cell line panel) under the *In Vitro* Cell-Line Screening Project (IVCLSP). Acute toxicity data were obtained in athymic nude mice (400, 200, 100 mg/kg bwt of PT19c, IP, 13 days) through the National Cancer Institute (NCI) Developmental Therapeutics Program. The details of NCI60 cell line screening and NCI acute toxicity assay can be found at http://dtp.nci.nih.gov.

Estimation of serum calcium levels in mice. All animal experiments were performed in the animal facilities of Rhode Island Hospital (RIH) with strict adherence to the guidelines of the Animal Welfare Committee of RIH and Women & Infants Hospital (AWC Protocol #0185-06; Laboratory Animal Protection Approval: A3922-01; CMTT: 0061-07) in accordance with the guidelines set by the NIH in the care and use of laboratory animals. Animal Welfare Committee (AWC Protocol #0185-06) recommended most humane euthanasia procedures were performed to ensure painless death of animals. Twelve-six-week-old female nude mice (NU/NU strain code 088/homozygous, 25 g average weight; Charles River Laboratories, Wilmington, MA) were randomly assigned to a control group (4 animals) or treatment group (8 animals). Vehicle (PBS/2.5% EtOH) or PT19c (10 mg/kg; $n = 4$) or calcitriol (10 μg/kg; $n = 4$) in 0.3 mL of vehicle was administered intraperitoneally every other day for 35 days. Blood was collected after cardiac puncture, and serum calcium levels were analyzed by IDEXX Laboratories Inc. (North Grafton, MA).

Determination of agonistic/antagonistic properties of PT19c using a VDR-coactivator binding assay. VDR modulation, both agonist and antagonistic, was determined by a fluorescence polarization assay.[19] Briefly, PT19c was serially diluted in DMSO and 100 nL of each concentration was transferred into 20 μL protein buffer 7.5 nM SRC2-3 (CKKKENALL-RYLLDKDDTKD) labeled with Alexa Fluor 647 Maleimide, and 1 μM VDR-LBD in the presence and absence of calcitriol (100 nM) in quadruplet using black 384 well plate (Costar, Cat No. 3658). The samples were allowed to equilibrate for 2 hours. Binding was then measured using fluorescence polarization (excitation 620 nm, emission 688 nm) using a M1000 plate reader (Tecan, Mannedorf, Switzerland). The experiments were evaluated using GraphPad Prism 5, and IC_{50} values were obtained by Sigmoidal dose-response-variable slope equation (4 parameters). Values are given as the mean values with a 95% confidence interval. For the antagonist assay CBT1 (20 μM) and DMSO and for the agonist assay calcitriol 100 nM and DMSO were used as positive and negative controls, respectively.

Morphological studies. Effect of PT19c on focal adhesion formation and actin filament organization in ovarian cancer (SKOV-3) cells was determined by fluorescence microscopy. SKOV-3 cells (1×10^4/chamber) were seeded into glass chambers (Nalge Nunc, Naperville, IL) and treated with EtOH or PT19c (2 μM) for 24 hours in complete DMEM media (Invitrogen, Cat No. 11995). The media was removed and the cells were washed with DPBS and fixed with cold 70% EtOH for 15 minutes. Ethanol was removed and the cells were washed with DPBS (2×5 mL) and stained with alexaflour-phalloidin (Invitrogen) for 30 minutes and then washed with DPBS (3×5 minutes). The images of multiple fields were taken with an inverted microscope (Nikon Eclipse TE2000-E, CCD camera) using 40× objective.

Epithelial ovarian cancer and endometrial cancer xenograft model in mice. Animal experiments were carried out in the animal facilities of Rhode Island Hospital (RIH),with strict adherence to the guidelines of the Animal Welfare Committee of RIH and Women and Infants Hospital of Rhode Island (Laboratory Animal Protection Approval: A3922-01; CMTT: 0061-07). Animal Welfare Committee (AWC Protocol #0185-06) recommended most humane euthanasia procedures were performed to ensure painless death of animals. Four-week-old immunodeficient nude mice (NU/NU; strain code 088/homozygous) (Charles River Laboratories) were maintained at a temperature of 22 ± 1°C and a relative humidity of 55 ± 5%, with a 12-hour light/dark cycle. SKOV-3 cells were cultured to 80% confluence in DMEM complete medium, harvested by trypsination, pooled in

complete medium, washed in PBS twice, and 2×10^6 cells/inoculate were suspended in 0.1 mL of matrigel and inoculated subcutaneously in the flank of mice. Similarly, hormone sensitive endometrial cancer cell-lines (ECC-1) were grown to 80% confluency, harvested, and 0.1 mL cell suspension of 1 million cells in Matrigel was inoculated subcutaneously in the left flank of the nude mice. Mice were randomly assigned at day 14 of tumor growth to control and experimental groups. PT19c solution in 100% EtOH was diluted 1:40 in PBS before administration in animals. Mice were treated intraperitoneally every other day with either vehicle control (control group; 8 animals) or 300 µL (10 mg/kg bwt) of PT19c (n = 8) for 35 days. Mice were weighed and tumor size calculated using a caliper every 5 days.

Molecular docking studies with VDR ligand binding domain

MDS was carried out using the AutoDock 4.0 program with the structure of PT19c and calcitriol-liganded VDR (PDB ID: 1DB1) provided by the Protein Data Bank.[20] For PT19c docking simulation, the ligand in the binding pocket of VDR was removed. MDS was carried out applying the Lamarckian genetic algorithm. A population size of 150 and 2,500,000 energy evaluations were used for 50 local search runs. The docking area was defined by a box, with grid spacing of 0.375 Å and the dimension of 50 × 50 × 50 points along the *x, y*, and *z* axes. The conformation with the lowest docked energy was chosen as a possible candidate for PT19c. Images of structures were generated using UCSF Chimera.

Acknowledgements

The authors thank Ginny Hovanesian for help with microscopy.

Declaration of Conflicting Interests

The author(s) declared the following potential conflicts of interest with respect to the research, authorship, and/or publication of this article: LB and RKS are listed as co-inventors on a pending patent application. Other authors do not express a conflict of interest.

Funding

The author(s) disclosed receipt of the following financial support for the research, authorship, and/or publication of this article: RGM and RKS are partially supported by a "Swim Across America" fund. RGM is also supported by NCI Grant RO1 CA136491-01.

References

1. Bouillon R, Okamura WH, Norman AW. Structure-function relationships in the vitamin D endocrine system. Endocr Rev. 1995;16:200-57.
2. Deeb KK, Trump DL, Johnson CS. Vitamin D signalling pathways in cancer: potential for anticancer therapeutics. Nat Rev Cancer. 2007;7:684-700.
3. Lambert JR, Young CD, Persons KS, Ray R. Mechanistic and pharmacodynamic studies of a 25-hydroxyvitamin D3 derivative in prostate cancer cells. Biochem Biophys Res Commun. 2007;361:189-95.
4. Osborn JL, Schwartz GG, Bahnson R, Smith DC, Trump DL. Phase II trial of oral 1,25-dihydroxyvitamin D (calcitriol) in hormone refractory prostate cancer. Urol Oncol. 1995;1:195-8.
5. Prudencio JN, Akutsu N, Benlimame T, *et al*. Action of low calcemic 1α,25 dihydroxyvitamin D3 analogue EB1089 in head and neck squamous cell carcinoma. J Natl Cancer Inst. 2001;93:745-53.
6. Kawa S, Yoshizawa K, Nikaido T, Kiyosawa K. Inhibitory effect of 22-oxa-1,25-dihydroxyvitamin D3, maxacalcitol, on the proliferation of pancreatic cancer cell lines. J Steroid Biochem Mol Biol. 2005;97:173-7.
7. Brard L, Lange TS, Robison K, *et al*. Evaluation of the first ergocalciferol-derived, non hypercalcemic anti-cancer agent MT19c in ovarian cancer SKOV-3 cell lines. Gynecol Oncol. 2011;123:370-8.
8. Brard L, Kalkunte S, Singh RK. Heterocyclic and derivatives thereof and methods of manufacture and therapeutic use. US patient WO/2007/070494. 2007 Jun 21.
9. Moore RG, Lange TS, Robinson K, *et al*. Efficacy of a non-hypercalcemic vitamin-D2 derived anti-cancer agent (MT19c) and inhibition of fatty acid synthesis in an ovarian cancer xenograft model. PLoS One. 2012;7(4):e34443.
10. Stuckey A, Fischer A, Miller DH, *et al*. Integrated genomics of ovarian xenograft tumor progression and chemotherapy response. BMC Cancer. 2011;11:308.
11. Bury Y, Stienmeyer A, Carlberg C. Structure-activity relationship of carboxylic ester antagonists of the vitamin D3 receptor. Mol Pharmacol. 2000;58:1067-74.
12. Morris GM, Goodsell DS, Halliday RS, *et al*. Automated docking using Lamarckian genetic algorithm and an empirical binding free energy function. J Comput Chem. 1998;19:1639-62.
13. Korch C, Spillman MA, Jackson TA, *et al*. DNA profiling analysis of endometrial and ovarian cell lines reveals misidentification, redundancy and contamination. Gynecol Oncol. 2012;127:241-8.
14. Maruyama W, Irie S, Sato TA. Morphological changes in the nucleus and actin cytoskeleton in the process of Fas-induced apoptosis in Jurkat T cells. Histochem J. 2000;32:495-503.
15. Walling EA, Krafft GA, Ware BR. Actin assembly activity of cytochalasins and cytochalasin analogs assayed using fluorescence photobleaching recovery. Arch Biochem Biophys. 1988;264:321-32.
16. Rao JY, Jin YS, Zheng Q, Cheng J, Tai J, Hemstreet GP. Alterations of the actin polymerization status as an apoptotic morphological effector in HL-60 cells. J Cell Biochem. 1999;75:686-97.
17. Yamazaki Y, Tsuruga M, Zhou D, Fujita Y, Shang X. Cytoskeletal disruption accelerates caspase-3 activation and alters the intracellular membrane reorganization in DNA damage-induced apoptosis. Exp Cell Res. 2000;259:64-78.
18. Suria H, Chau LA, Negrou E, Kelvin DJ, Madrenas J. Cytoskeletal disruption induces T cell apoptosis by a caspase-3 mediated mechanism. Life Sci. 1999;65:2697-707.
19. Teichert A, Arnold LA, Otieno S, *et al*. Quantification of the vitamin D receptor-coregulator interaction. Biochemistry. 2009;48:1454-61.
20. Berman HM, Westbrook J, Feng Z, *et al*. The protein data bank. Nucleic Acids Res. 2000;28:235-42.